Volume 15, Issue 3, 152525 (1-14)

Journal of Rangeland Science (JRS)

https://doi.org/10.57647/j.jrs.2025.1503.25

Assessment of land surface temperature anomaly and its effects on dust storm index anomaly over southeastern rangeland of Iran

Maede Nasry[1], Mohammad Rahimi[1,*], Hadi Jalili[2], Farzaneh Hadadi[2], Ali Akbar Damavandi[3]

[1]*Combat to Desertification Department, Faculty of Desert Studies, Semnan University, Semnan, Iran.*
[2]*Iranian Space Research Institute, Tehran, Iran.*
[3]*Institute of Agricultural Education and Extension, Agricultural Research, Education and Extension Organization (AREEO), Tehran, Iran.*

[*]**Corresponding author:** mrahimi@semnan.ac.ir

Original Research

Received:
12 December 2023
Revised:
12 August 2024
Accepted:
13 September 2024
Published online:
20 July 2025

Abstract:

Dust storms are frequent events in the southeastern parts of Iran. The rangelands play a crucial role in the socio-economic conditions of rural populations and control soil erosion in southeast Iran. Spatial-temporal changes in terrestrial parameters such as land surface temperature controlled dust storm activity processes. Therefore, gathering frequent information about the Land Surface Temperature Anomaly (LSTA) and its relationship with Dust Storm index Anomaly (DSIA) was the aim of this study. Moderate Resolution Imaging Spectroradiometer (MODIS) products were used to monitor LSTA. The dataset was composed of MOD11A2 product, which provides a value with 1000-m spatial resolution and 8-day temporal resolution from February and October (2000 – 2020). ENVI 5.6 software was used for the image misacting and reprojection of satellite images. For the determination of the DSIA, three-hour recordings (8 times a day) of the synoptic codes (07, 08, 09, 30 to 35, and 98) related to dust and visibility were used at the 8 meteorological stations. Annual mean DSIA values were computed in Excel 2016 software. Spatial maps of LSTA and DSIA were drawn in ArcGIS 10.2.2. The Pearson correlation coefficients were computed to examine the correlation between LSTA and DSIA. Results demonstrate that the lowest annual LSTA values were observed in the years 2000, 2001, 2012, 2014, 2019, and 2020. The highest annual LSTA values were observed in 2008, 2006, 2007, 2015, and 2018. The DSIA and LSTA time series had decreasing trends. A positive correlation between LSTA and DSIA ($p < 0.05$) was observed. The results imply that positive LSTA increases dust storms in the southeastern parts of Iran. Limited adaptive capacity, lack of information, and poor stakeholder coordination and cooperation caused the large-scale impact of the dust storms. These results can be useful for the decision-makers in assessing the risks of dust storm impacts and reducing their negative consequences in the southeastern rangelands of Iran.

Keywords: Dust storm, Dryland, Hazard, MODIS, 120-day winds

Introduction

The southeastern region of Iran is one of the most active sources of dust storms in Asia, and dust events occur in this region almost all year round (Abbasi et al., 2018), but their frequency is higher in summer and spring seasons, which corresponds to the 120-day winds blowing (Rashki et al., 2017). Dust storms are a frequent natural hazard to the socioeconomic systems of southeastern Iran (Namdari et al., 2021). As a hazard, dust and sand storms have detrimental effects on rangelands, livestock revenue, and physical production in dry lands (figure 1) (Kang et al., 2021). For many rural dryland populations of southeast Iran, pastoralists remain the only viable livelihood (Abdollahi et al., 2023). Dust particles deposited on vegetation interrupting photosynthesis and respiration, and stomata clogging in many ways (Zeidali et al., 2015). Therefore, dust reduces vegetation production and economically im-

Figure 1. Dust storm events in rangelands and rural areas of southeast Iran.

poses substantial losses. On the other hand, because of livestock dependence on the rangelands to provide forage indirectly losses of rangeland production can reduce land productivity. High concentrations of dust may lead to weak livestock immune systems expose livestock to infectious diseases and bacteria and eventually cause death (Moradi and Alamizadeh, 2012).

Land surface characteristic changes have impacts on the frequency and intensity of wind erosion (Leys John et al., 2022). Considering the close link between wind erosion and dust storms, determining the major factors influencing dust erosion is an essential phase in any effort to reduce the frequency and intensity of dust storms. As a physical characteristic of the earth's surface, Land Surface Temperature (LST) is an important factor controlling the soil surface processes (Hussain et al., 2019).

It is described as the temperature of the surface which refers to soil surface temperature for bare soil, and canopy surface temperature of vegetation for densely vegetated ground (Darvishi Boloorani et al., 2021). LST combines the results of energy fluxes between the atmosphere and the ground and surface-atmosphere interactions so affects the physics of land-surface processes (Fathizad et al., 2017).

Soil moisture by increasing the adhesion between the soil particles increases the resistance of the soil to wind erosion (Hashemi et al., 2022). LST has been identified as a good indicator of moisture conditions because it is sensitive to water changes. Increasing LST causes the enhanced evapotranspiration, subsequently leading to wind erosion and the transfer of separated soil particles to the atmosphere (Alsubhi et al., 2022). Therefore, LST has an important role in preventing wind erosion (Damavandi et al., 2016). LST measures the emission of thermal radiance from the land surface where the incoming solar energy interacts with and heats the ground (Alsubhi et al., 2022). Various methodologies have been developed to calculate LST from space-based data. Remote-sensing indices can provide a valuable source of data for different scales at a low cost on time. Moderate Resolution Imaging Spectroradiometer (MODIS) is widely used in terms of spatial and temporal evaluation of LST (Darvishi Boloorani et al., 2021).

During the formation of dust storms, the passage of wind currents at a speed higher than the threshold over dry and destroyed lands causes the production of large masses of dust particles that reduce the horizontal visibility to less than 1 km (Hashemi et al., 2022). One of the common methodologies for investigating the trend of spatiotemporal variations in dust storm activity is ground-based indices. Dust Storm Index Anomaly (DSIA) also is used to analyze the temporal and spatial dust storm events.

Mu et al. (2013) indicated that long-term dust storms affect livestock in Mongolia in spring. It results in mass livestock death and economic loss.

Ahmadi et al. (2024) demonstrated that dust storms affect pastoralists' livelihoods in West of Iran. These effects include the decreased growth of grassland, the plant leaf pollution, and the reduced grazing.

There are many studies in the background of dust storm impacts; however, there are few studies on the DSIA, and there is a gap that this study tries to fill. Examining the correlations between the DSIA and the LSTA in the rangelands of southeast Iran is the novelty and unique aspect of this study. The objective of this study was to identify the long-term spatiotemporal variations in the LST and DSIA over the southeast rangelands of Iran.

Materials and methods

Study area

The present study covers the parts of the Sistan and Baluchistan, Kerman, and Hormuzgan-Iran provinces (figure 2). Resolution Imaging Spectroradiometer (MODIS) is a sensor onboard the two Terra and Aqua satellite platforms launched by National Aeronautics and Space Administration (NASA) (Hassan et al., 2018). MODIS covers Iran in 4 tiles and the tile h 22v06 covers the southeastern part of Iran, each tile covers an area of 2330 km. Therefore, the study area has been selected based on the coverage boundaries of the satellite frame in the area.

Sistan and Baluchistan province

The Sistan and Baluchistan are located in the southeastern Iranian borders with Afghanistan and Pakistan. Whole Sistan and Baluchistan which is only 180,720 Km^2, lie between 30°50′N-31°28′N latitudes and 61°15′E-61°50′E longitudes. Aridity is the main characteristic of this region and dust storms are extremely affecting Sistan and Baluchistan

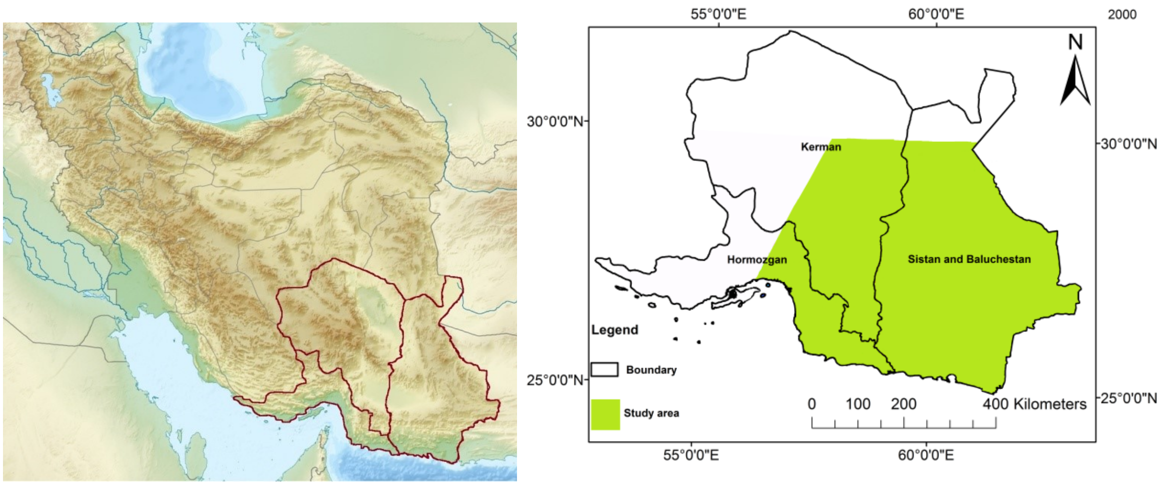

Figure 2. The location of the study area in Iran and three provinces including Sistan and Baluchistan, Kerman, and Hormuzgan provinces, Iran.

throughout the year. In this region, annual precipitation (55 mm) significantly occurs in winter (December to February), and the mean annual temperature is 22 °C.

Kerman province

Kerman province can be characterized as an arid and semi-arid region with a hot and dry summer, and precipitation during winter. It is located in the southeast of Iran between 26°29′N and 31°58′N latitudes and 54°21′E and 59°34′E. Kerman province covers an area of 183,193 km^2. In this area, precipitation is strongly seasonal (155 mm) and the annual average temperature is 15.8 °C.

Hormuzgan province

Hormuzgan Province is situated in the southeast of Iran and borders the northern part of the Persian Gulf facing the United Arab Emirates and Oman. It is located between about 52°–59° E and 25°–28° N and has 1000 km (620 miles) of coastline and covers an area of 71,193 km^2. About 54% of the Hormuzgan area is a coastal desert. The annual average temperature and precipitation are 27 °C and 215.8 mm, respectively.

Data collection

In this study, the satellite imagery dataset was created using LST products (Mod11A2) that have been collected from February to October (growing season) over 21 years (2000 – 2020). These products were obtained from the national aeronautics and space administration earth observing system dataset and information system (https://ladsweb.modaps.eosdis.nasa.gov). LST products are downloaded from the Land Processes Distributed Active Archive Center (LP DAAC) website using the NASA Warehouse Inventory Search Tool (WIST). The downloaded data have been then analyzed using Geographic Information System (GIS) tools in ArcGIS software. The meteorological datasets include daily maximum dust codes and daily visibility data provided by the Iran Meteorological Organization (IMO) (https://irimo.ir/far/index.php) obtained from the 8 meteorological stations distributed in the study areas in the same period as satellite imagery.

Anomaly definition

Anomalies are the differences between individual months or years and some long-term averages that are often used in analyzing climate change. Anomalies are more important than absolute values. Data points that are inconsistent with the major data distribution are called anomalies. Positive anomaly means that the observed value was more than the baseline and negative anomaly was less than the baseline (Ebrahimi-Khusfi et al., 2020).

Calculations of DSIA

In this study, a meteorological dataset from 8 weather stations was used to analyze long-term variations in DSIA during the 2000 – 2020 periods.

Although there are many dust storm activity indices based on meteorological observations, the DSI proved that is an accurate index for monitoring dust storms. To calculate Dust Storm Index Anomaly (DSIA), the first step is to assess monthly and annual DSI values.

For this, DSI has been obtained using visibility data and dust codes. All types of maximum dust codes of Local Dust Events (LDE), Moderate Dust Storms (MDS), and Severe Dust Storms (SDS) were taken into account by defining a Dust Storm Index (DSI). According to the World Meteorological Organization (WMO), dust codes 07 – 09, 31 – 35, and 98 can be used to calculate the DSI. Monthly and annual DSI values for the stations are calculated using the following expressions (1) and (2) (Nanzada et al., 2019):

$$\mathrm{DSI}_{\mathrm{monthly}} = \sum_{i=1}^{n} [(0.05 \times \mathrm{LDE}) + \mathrm{MDE} + (5 \times \mathrm{SDS})] \quad (1)$$

$$\mathrm{DSI}_{\mathrm{annual}} = \sum_{1}^{9} \mathrm{DSI}_{\mathrm{monthly}} \quad (2)$$

where:

LDE is defined by codes 07, 08, and 09;

MDS is known by codes 30, 31, 32, and 98; and

SDS is specified by codes 33, 34, and 35 (Nanzada et al., 2019).

The long-term DSI (DSIlt) was calculated using the following equation (3) (Nanzada et al., 2019):

$$\mathrm{DSI}_{\mathrm{lt}} = \sum_{1}^{21} \frac{\mathrm{DSI}_{\mathrm{annual}}}{21} \tag{3}$$

DSIA can be calculated by the following equation:

$$\mathrm{DSIA} = \frac{\mathrm{DSI}_{\mathrm{annual}} - \mathrm{DSI}_{\mathrm{lt}}}{\mathrm{DSI}_{\mathrm{lt}}} \times 100 \tag{4}$$

We divided DSIA values into two positive and negative categories. When the long-term mean value of DSI is less than the annual dust storm index, DSIA is positive (DSIA $>$ 0), and when it is higher than the annual dust storm index, DSIA is negative (DSIA $<$ 0).

Calculations of LSTA

Monitoring LSTA is the most suitable approach for investigating the LSTA effect on the DSIA. To calculate LSTA, the monthly LST for each year (Feb-Oct) has been first assessed by the following expression (Nanzada et al., 2019).

$$\mathrm{LST}_{\mathrm{mean}} = \frac{\mathrm{LST}_1 + \mathrm{LST}_2 + \ldots + \mathrm{LST}_\mathrm{n}}{\mathrm{n}} \tag{5}$$

where:
$\mathrm{LST}_{\mathrm{mean}}$ is the mean LST values of February to October of *i* year.
LST_1 is the first and LST_n is the last 8-days of LST values from February to October of the year.
After computing $\mathrm{LST}_{\mathrm{mean}}$ during the 21 years, the long-term values were then estimated using the following expression (Nanzada et al., 2019):

$$\mathrm{LST}_{\mathrm{lt}} = \sum_{i=1}^{21} \frac{\mathrm{LST}_{\mathrm{annual}}}{21} \tag{6}$$

The LSTA was estimated using the following expression: 2019):

$$\mathrm{LST}_{\mathrm{anomaly}} = \frac{\mathrm{LST}_{\mathrm{annual}} - \mathrm{LST}_{\mathrm{lt}}}{\mathrm{LST}_{\mathrm{lt}}} \times 100 \tag{7}$$

where:
LSTA *i* is the LSTA for the growing season during *i* year.
Correlation between LSTA and DSIA was the estimates using Pearson correlation.
The flowchart of methodology is presented in figure 3.

Results

Temporal variations in LSTA between the years 2000 – 2020

The temporal distribution of the LST and DSI anomaly values during the period of 2000 – 2020 are plotted in figure 4. The plots are labeled by the names of the stations. LSTA values were reclassified into two categories, greater and smaller than zero. The positive LST anomalies (LSTA $>$ 0) show that the annual LST was higher than the long-term mean value of LST, while negative LSTA (LSTA $<$ 0) indicates that the annual LST value was less than the long-term average amount of LST. The sharp LSTA-reduction values were observed over Bam, Iranshahr, Minab, Zahedan, and Khash from 2015 to 2020. The LSTA-reduction trends were slight over the Chabahar, Kahnuj, and Banndarabas stations. The highest interannual LSTA values were observed for Bam and Kahnuj stations in 2008, Banndarabas and Kahnuj stations in 2007, and Chabahar, Iranshahr, and Minab in 2000 and 2001. In contrast, the lowest annual LSTA values were observed in 2012, 2014, 2018, and 2020.

Temporal variations in DSIA between the years 2000 – 2020

Interannual variations in the DSIA values for each station during 2000 – 2020 are shown in figure 5. The plots are labeled by the names of the stations. DSIA values were reclassified into two categories, greater and smaller than zero. The positive DSIA (DSIA $>$ 0) show that the annual DSI was higher than the long-term mean value of LST, while negative LSTA (DSIA $<$ 0) indicates that the annual LST value was less than the long-term average amount of DSI. The negative DSIA (DSIA $<$ 0) value was observed over

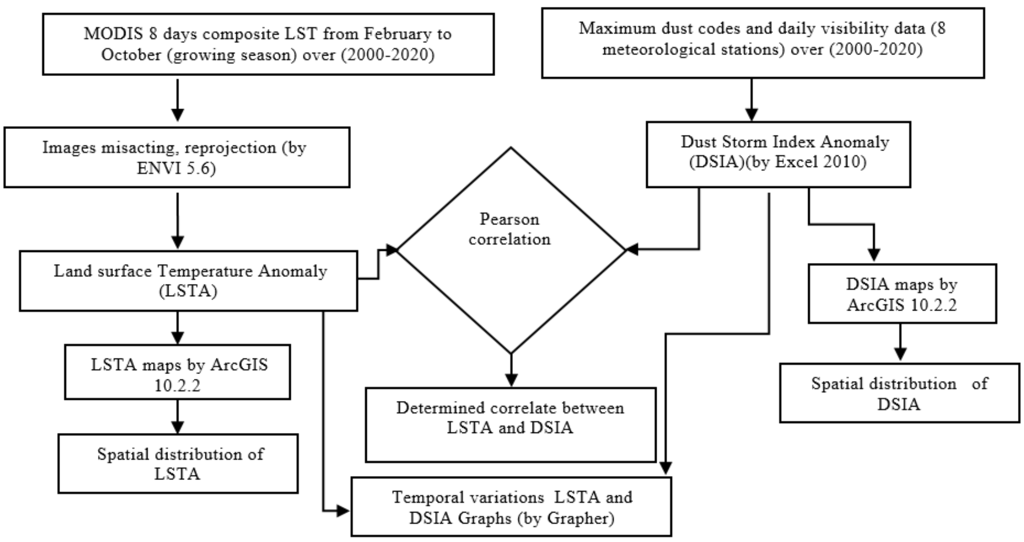

Figure 3. Flowchart of methodology.

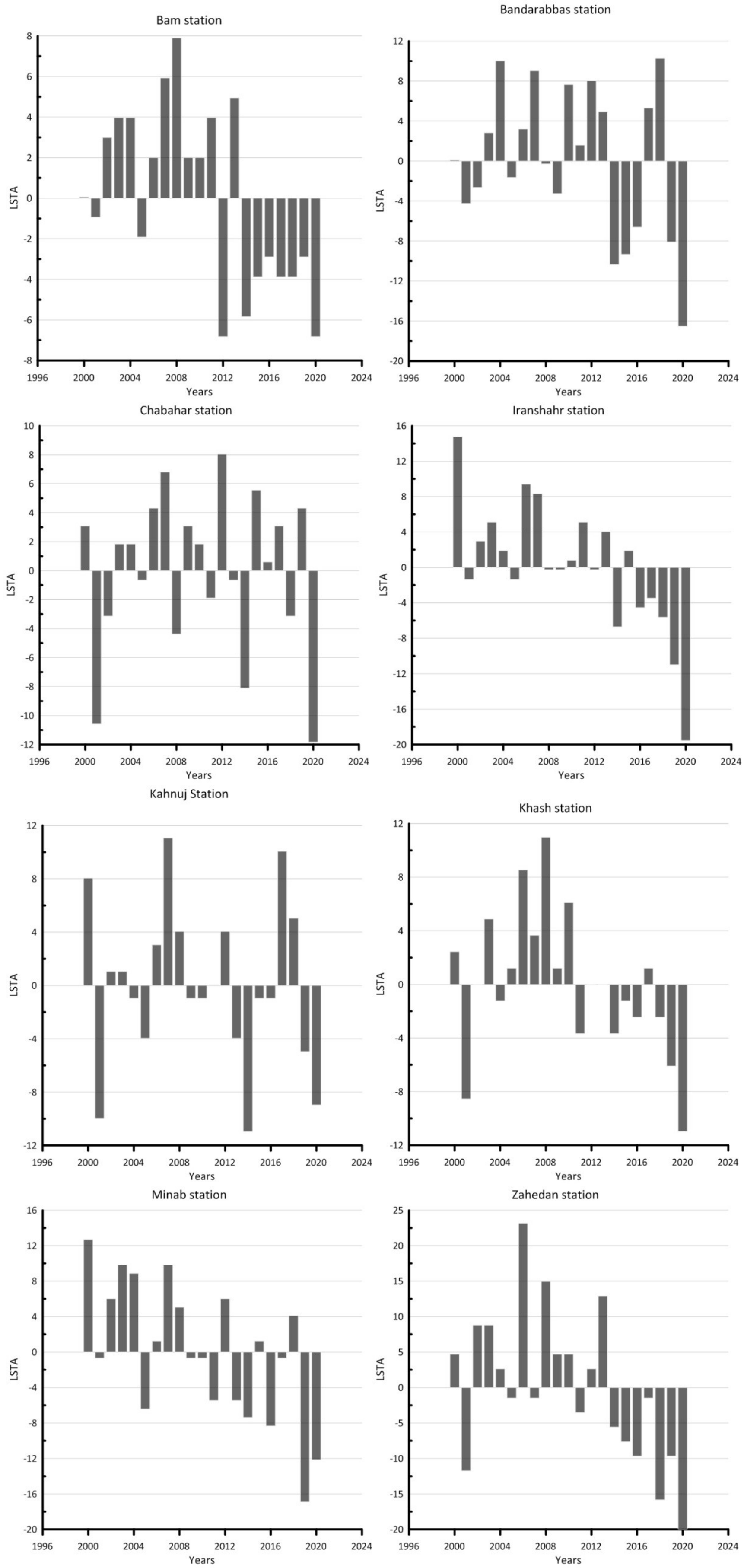

Figure 4. Interannual variation in the LSTA values 2000 – 2020.

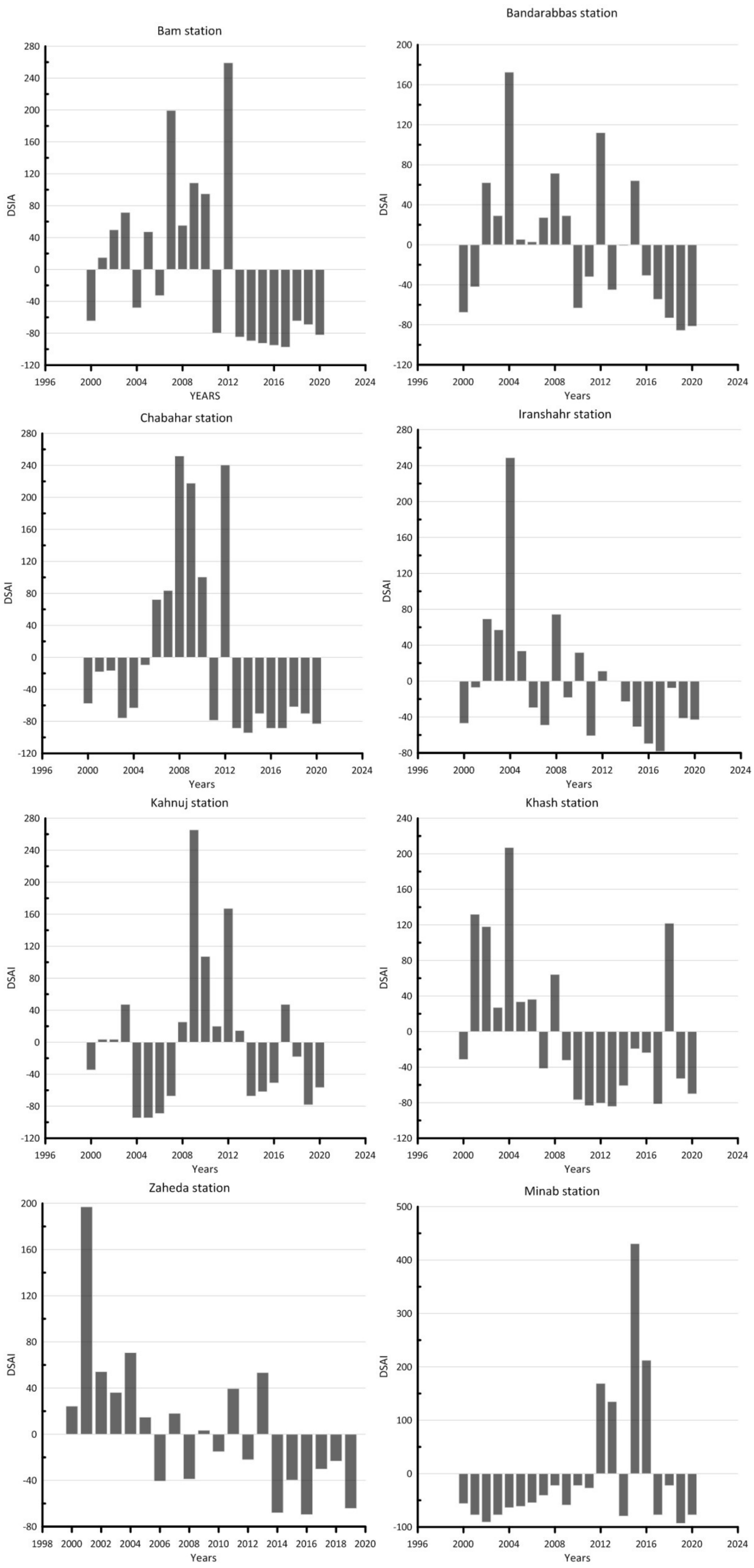

Figure 5. Interannual variation in the DSIA values 2000 – 2020.

the Bam, Banndarabas, Chabahar, Iranshahr, Khash, and Zahedan stations from 2015 to 2020. The negative DSIA (DSIA < 0) was slight over the Kahnuj stations. However, the DSIA (DSIA < 0) value has been positive in Minab station in recent years. Results demonstrate that the years 2001, 2004, 2008, 2009, 2012, and 2015 were the most affected years by dust activity in most of the stations. In contrast, the years 2000, 2002, 2004, 2010, 2016, 2017, and 2019 were less active.

Correlation between DSIA and LSTA

The correlation analysis indicated that LSTA was significantly correlated with DSIA. Strong positive correlations were demonstrated between LSTA and DSIA ($r = 0.52$, pvalue < 0.05).

DSIA mapping

In the following section, the DSIA maps have been generated (figure 6). The DSIA maps are labeled by the years $(2000-2020)$. In the maps, the colors change from red to blue meaning the highest DSIA values to the lowest DSIA values. It can be seen that dust storm activities decline by moving from the eastern parts of the region to the west. DSIA values range from -95 to $+265$. The northeastern region has been almost always prone to dust production. In some years, such as 2006 to 2010, according to the values

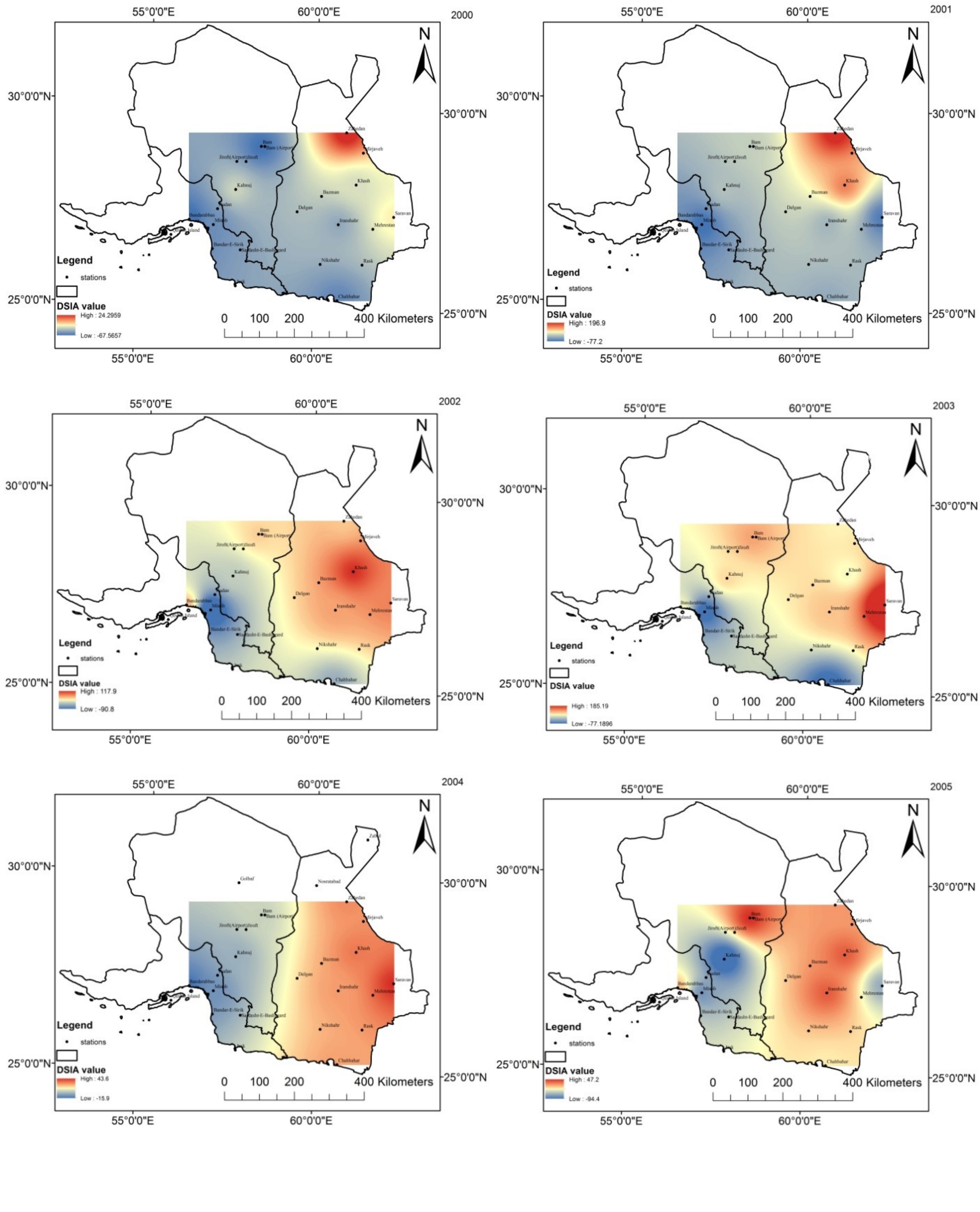

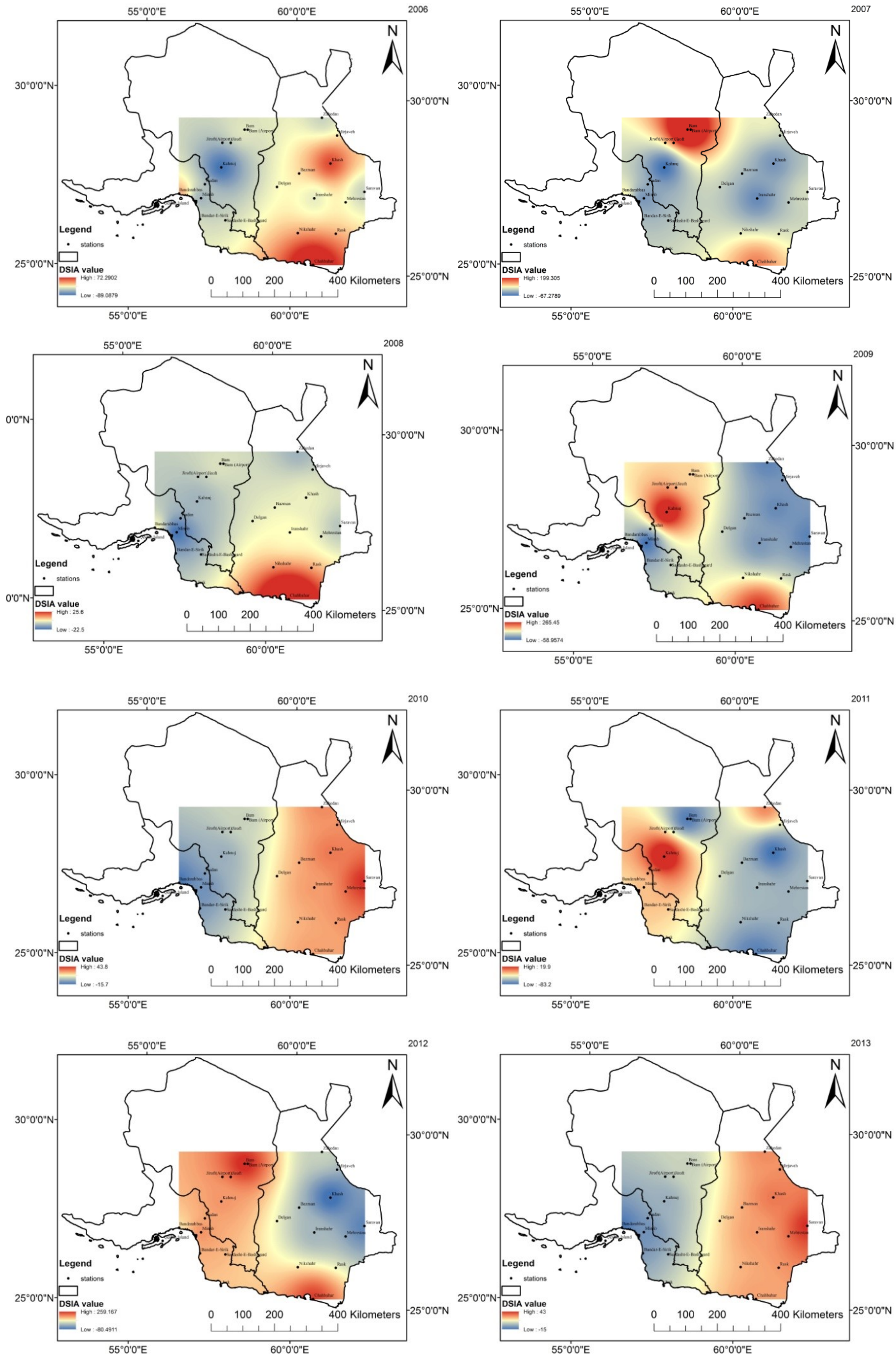

2006
Legend
stations
DSIA value
High : 72.2902
Low : -89.0879
2007
High : 199.305
Low : -67.2789
2008
High : 25.6
Low : -22.5
2009
High : 265.45
Low : -58.9574
2010
High : 43.8
Low : -15.7
2011
High : 19.9
Low : -83.2
2012
High : 259.167
Low : -80.4911
2013
High : 43
Low : -15
0 100 200 400 Kilometers
55°0'0"E
60°0'0"E
30°0'0"N
25°0'0"N
N

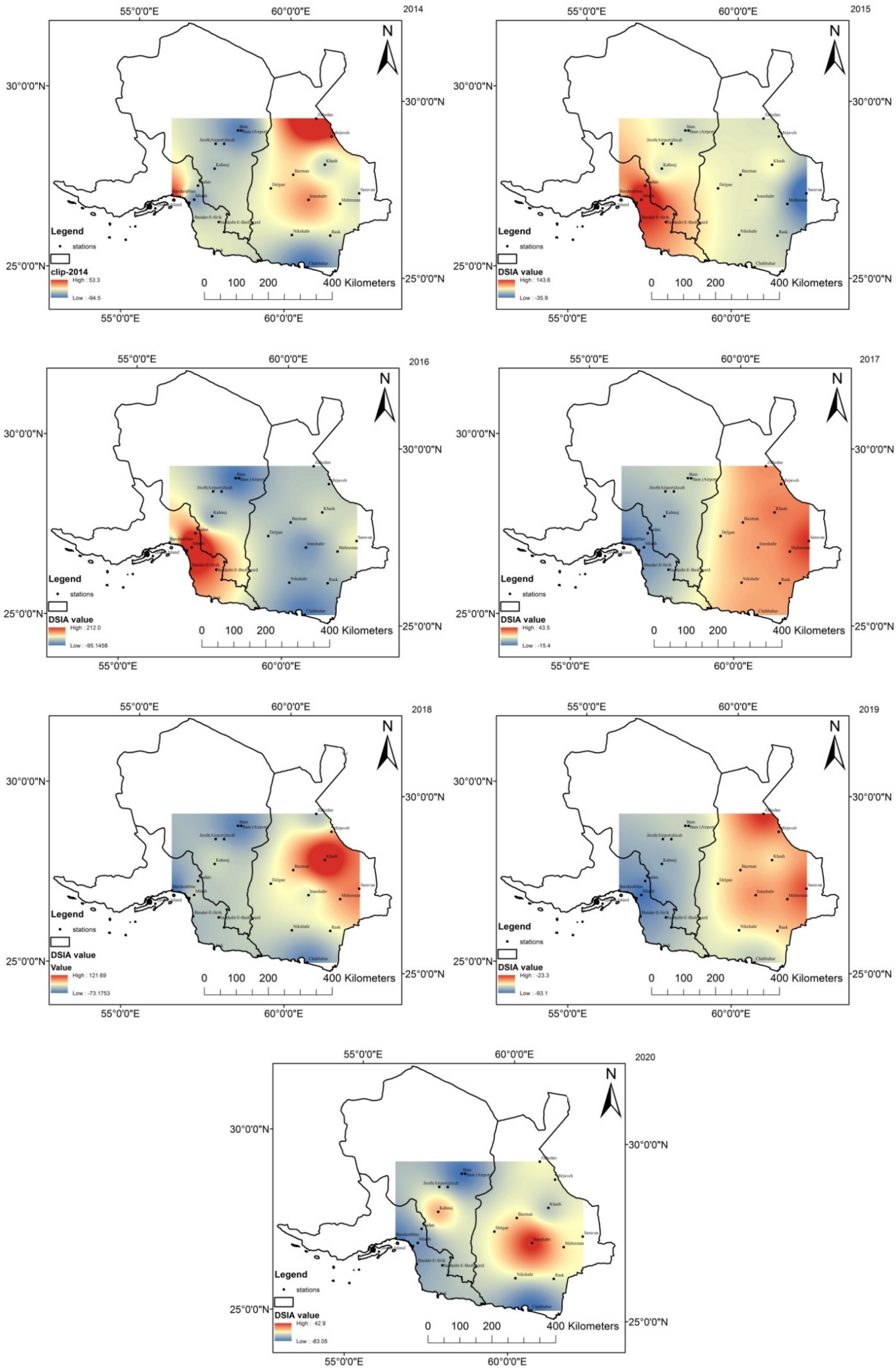

Figure 6. Spatial distribution of DSIA for 2000 – 2020 in the southeast of Iran.

of DSIA > 0, the southern parts have also seen an increase in dust storms. In some years, the intensity of dust activity has been very high, which had caused the entire region to be involved in the production of dust storms in 2005, 2006 and 2020. On the other hand, the areas with low values of DSIA < 0 are marked with light color. The southern and southwestern parts of the region are in better conditions in terms of dust storm activities in most years of the statistical period.

LSTA mapping

In this study, we used MODIS imagery from 2000 to 2020 to generate LSTA maps of spatial scales. The spatial distribution of LSTA trend is indicated in figure 7. The maps are labeled by the years $(2000-2020)$. In the maps, the colors change from brown to white meaning the highest LSTA values to the lowest LSTA values. The two major regions with the highest LSTA value were north to central rangeland areas. The LSTA values generally were low across northwest to southwest. Results showed LSTA values increased in parts of the east.

Discussion

In this study, the long-term spatiotemporal trends in the LSTA and dust DSIA were investigated. The LSTA temporal patterns showed that the lowest annual LSTA values were observed in the years 2000, 2001, 2012, 2014, 2019, and 2020. The highest annual LSTA values were observed

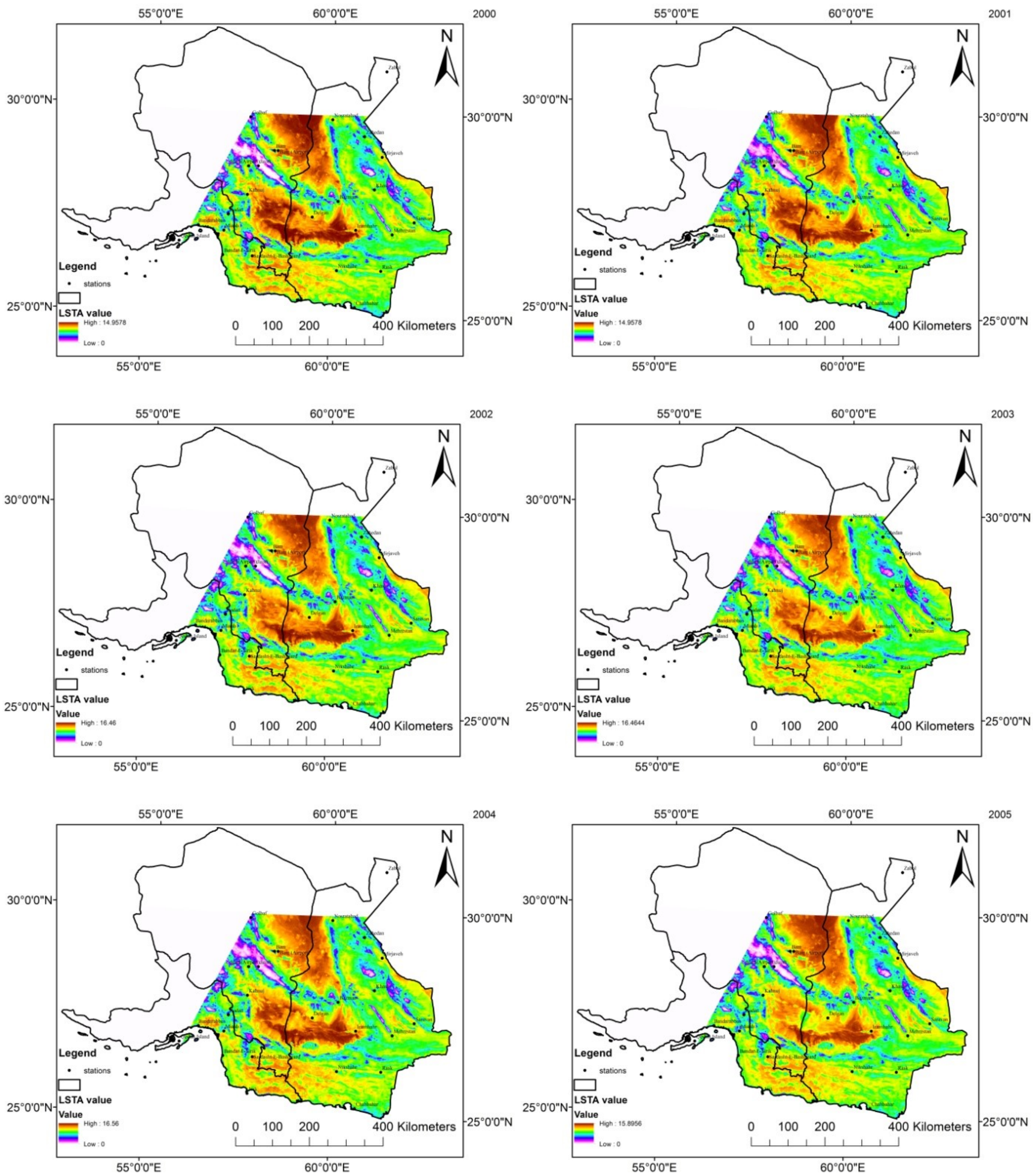

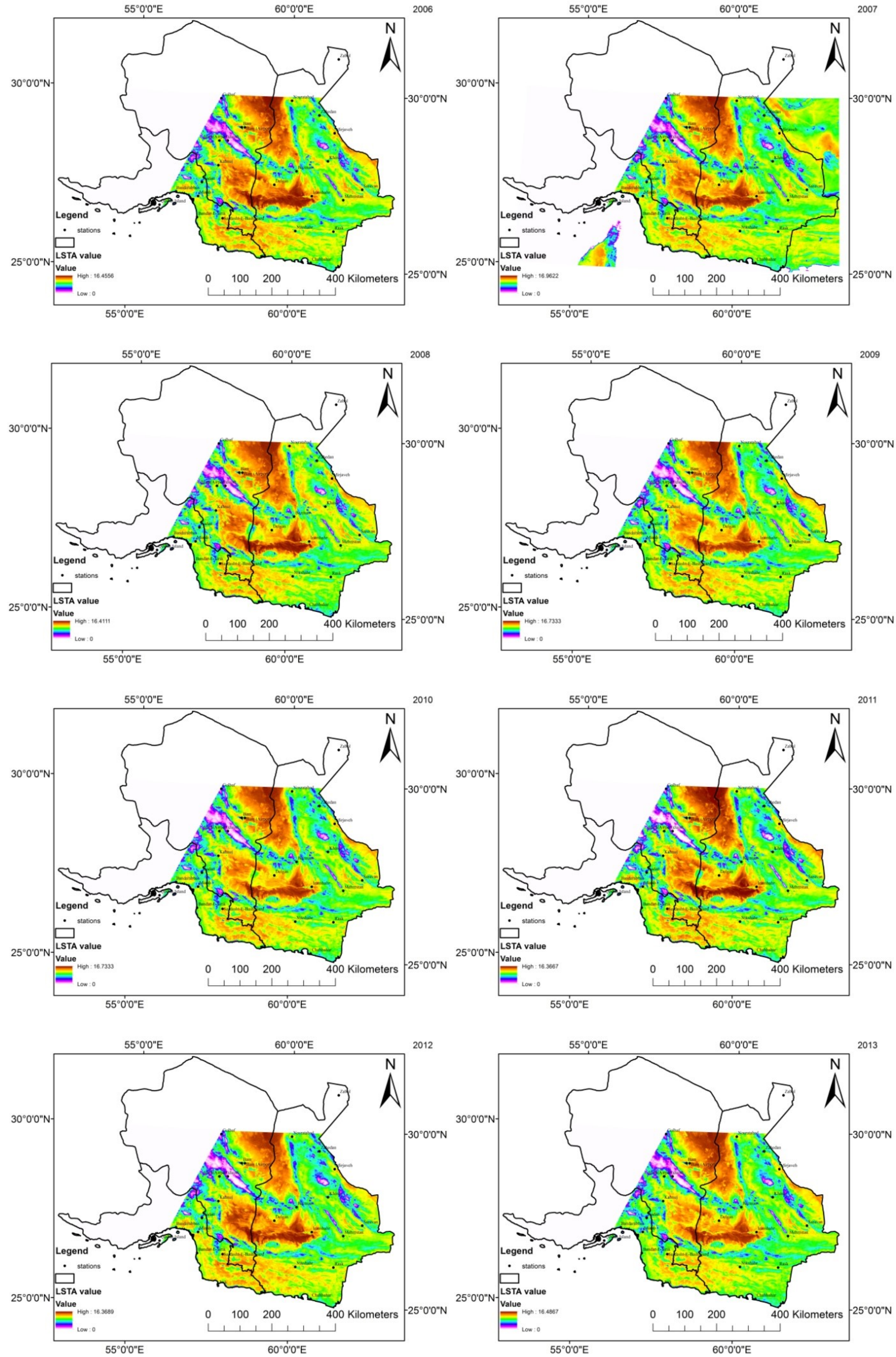
2006
55°0'0"E
60°0'0"E
30°0'0"N
25°0'0"N
N
Legend
stations
LSTA value
Value
High : 16.4556
Low : 0
0 100 200 400 Kilometers
2007
High : 16.9622
Low : 0
2008
High : 16.4111
Low : 0
2009
High : 16.7333
Low : 0
2010
High : 16.7333
Low : 0
2011
High : 16.3667
Low : 0
2012
High : 16.3689
Low : 0
2013
High : 16.4867
Low : 0

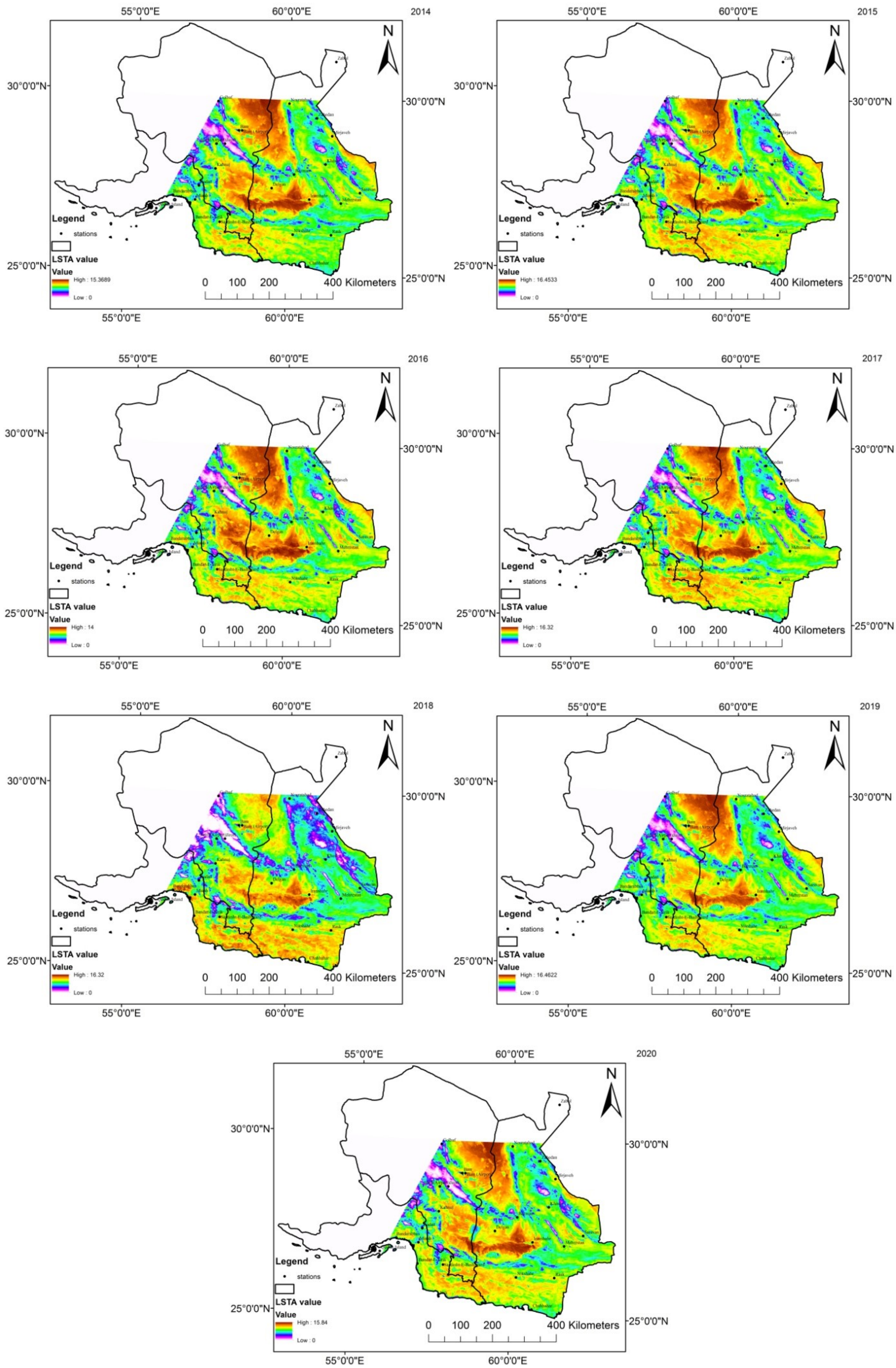

Figure 7. Spatial distribution of LSTA for 2000 – 2016 in the southeast of Iran.

in years in 2008, 2006, 2007, 2015, and 2018.

DSIA temporal patterns showed that the lowest annual DSIA values were observed in the years 2002, 2014, 2017, and 2017, and the highest annual DSIA values were observed in the years 2001, 2004, 2008, 2009, 2012, and 2015. Results demonstrate that LSTA had a reduction trend. Therefore, the land surface temperature had decreased in recent years. The results showed the DSIA and LSTA time series had decreasing trends. In this research, the positive correlation between LSTA and DSIA was the main hypothesis. The results indicate strong positive correlations between LSTA and DSIA; therefore, the hypothesis was proved.

We found that in the southeastern rangelands of Iran in recent years, LSTA and DSIA had a decreasing trend. Ebrahimi-Khusfi and Roustaei (2018) found a significant spatial correlation between LSTA and DSIA ($P < 0.05$) in western Iran. Qiao et al. (2021) monitored Fractional Vegetation Coverage (FVC) and LST to determine the degree of desertification and dust in the Horqin Sandy Land in China. Their results demonstrate a negative correlation between the FVC and the LST. LST by controlling soil moisture storage can directly affect soil particle resistance and indirectly the vegetation conditions.

The inverse relationship between LST and soil moisture leads to LST also indirectly affecting vegetation coverage in rangelands. Therefore, our results suggest that the decreased LST can stabilize rangeland vegetation conditions. Similar to our finding, Ebrahimi-Khusfi and Soleimani Sardoo (2021) reported that changes in the LST were the most important factor affecting wind erosion in the Zabol and southeastern parts of Iran.

Vegetation coverage in rangelands protects the soil and plays an important role in reducing wind erosion. Our results also revealed that in the eastern and southern parts of the study area, LSTA had significant changes coupled with higher land surface temperature. The intensity and magnitude of DSIA changes are positive in the northeast, eastern, and southeast parts of the region which indicates an increasing dust storm activity. Zeidali et al. (2015) showed that dust reduces livestock production and has the devastating impact on it.

Conclusion

This paper investigated the correlations between the DSIA and LSTA in the rangelands of southeast Iran. The results imply that positive LST anomalies increase dust storms in southeast Iran. Limited adaptive capacity, lack of information, and poor stakeholder coordination and cooperation caused the large-scale impact of the dust storms.

These results can be useful for decision-makers to assess the risks of dust storm impacts and reduce its negative consequences in the southeast rangelands of Iran. Future policies for mitigating the adverse effects of dust storms on rangeland need to be participatory while mitigating the impacts for promoting soil erosion. Also, short-term periods of fewer than 20 years of data in some stations, and missing daily visibility data were the limitations in this research. As a part of future research, an analysis of the potential correlation between DSIA and climate factors could be considered.

Authors Contributions
All authors have contributed equally to prepare the paper.

Availability of Data and Materials
The data that support the findings of this study are available from the corresponding author upon reasonable request.

Conflict of Interests
The authors declare that they have no known competing financial interests or personal relationships that could have appeared to influence the work reported in this paper.

References

Abbasi H.R., Opp C., Groll M., Rohipour H., Khosroshahi M., Khaksarian F., Gohardoust A. (2018) Spatial and temporal variation of the aeolian sediment transport in the ephemeral Baringak Lake (Sistan Plain, Iran) using field measurements and geostatistical analyses. *Geomorphol* 61 (4): 315–326.

Abdollahi K., Naghipour-Borj A.A., Bayati S., Eslami Z., Weston Black F. (2023) Assessment of Fire Effect on Water Balance Components under Different Land Uses in Central Zagros Rangelands, Iran. *Journal of Rangeland Science* 13 (4): 1–10.

Ahmadi F., Zamani O., Mirzaei H., Azadi H. (2024) Exploring the impact of dust storms on pastoralists' livelihoods in West Iran: Social, economic, and environmental consequences. *Environmental Quality Management* 33 (4): 821–833.

Alsubhi Y., Qureshi S., Assiri M.E., Siddiqui M.H. (2022) Quantifying the Impact of Dust Sources on Urban Physical Growth and Vegetation Status: A Case Study of Saudi Arabia. *Remote Sens* 14:25701.

Damavandi A.A., Rahimi M., Yazdani M.R., Noroozi A.A. (2016) Assessment of Drought Severity Using Vegetation Temperature Condition Index (VTCI) and Terra/MODIS Satellite Data in Rangelands of Markazi Province, Iran. *Journal of Rangeland Science* 6 (1): 121–142.

Darvishi Boloorani A., Najafi M.S., Mirzaie S. (2021) Role of land surface parameter change in dust emission and impacts of dust on climate in Southwest Asia. *Nat Hazards* 109:111–113.

Ebrahimi-Khusfi Z., Mirakbari M., Ebrahimi-Khusfi M., Taghizadeh-Mehrjardi R. (2020) Impact s of vegetation anomalies and agricultural drought on wind erosion over Iran from 2000 to 2018. *Appl Geogr* 125 (10): 102330.

Ebrahimi-Khusfi Z., Roustaei F. (2018) Dust storm index anomaly for sand-dust events monitoring in western Iran and its association with the NDVI and LST anomalies. *Environ Sci Pollut Res Int* 29 (8): 11101–11115.

Ebrahimi-Khusfi Z., Soleimani Sardoo M. (2021) Recent changes in physical properties of the land surface and their effects on dust events in different climatic regions of Iran. *Arabian Journal of Geosciences* 14:287.

Fathizad H., Mahdi T., Kalantari S., Shojaei S. (2017) The investigation of spatiotemporal variations of land surface temperature based on land use changes using NDVI in southwest of Iran. *Jour. Afr. Earth Sci* 134:249–256.

Hashemi Z., Soodaei zadeh H., Mohammad Hossein Mokhtari M.H. (2022) Investigation of the Relationship between Land Surface Temperature with Vegetation and Surface Moisture in the Land Use of Zahak Area of Sistan Plain Using Landsat Satellite Images. *Journal of Remote Sensing & GIS* 14 (1): 21–42.

Hassan G., Brouillette-Alarie S., Seraphin A., et al. (2018) Exposure to Extremist Online Content Could Lead to Violent Radicalization: A Systematic Review of Empirical Evidence. *International Journal of Developmental Sciences* 12:1–18.

Hussain S., Mubeen M., Akram W., Ahmad A., Habib-Ur-Rahman M., Ghaffar A., Amin A., et al. (2019) Study of land cover/land use changes using RS and GIS: a case study of Multan district, Pakistan. *Environ Monit Assess* 192 (1): 2.

Kang S., Lee S.H., Cho N., et al. (2021) Dust and sandstorm: ecosystem perspectives on dry land hazards in Northeast Asia: a review. *Jour. Ecology Environ* 45 (2): 25.

Leys John H.S., White S., Guerschman J., Strong C. (2022) Dust-storm frequencies, community attitudes, government policy, and land management practices during three major droughts in New South Wales, Australia. *The Rangeland Journal* 44:343–355.

Moradi P., Alamizadeh H. (2012) Dust phenomenon and methods of prevention, control and locking of agriculture and livestock production with emphasis on Khuzestan province. *The first National Conference on Health, Safety and Environment, Islamic Azad University of Mahshahr*

Mu H., Otani S., Shinoda M., Yokoyama Y., Onishi K., Hosoda T., Okamoto M., Kurozawa Y. (2013) Long-term effects of livestock loss caused by a dust storm on Mongolian inhabitants: a survey 1 year after the dust storm. *Yonago Acta Med* 56 (1): 39–42.

Namdari S., Valizadeh Kamran K., Sorooshian A. (2021) Analysis of some factors related to dust storms occurrence in the Sistan region. *Environ Sci Pollut Res Int* 28 (33): 45450–45458.

Nanzada L., Zhanga J., Battsetseg Tuvdendorj B., Nabila M., Zhanga S., Baia Y. (2019) NDVI anomaly for drought monitoring and its correlation with climate factors over Mongolia from 2000 to 2016. *Journal of Arid Environments* 164:69–77.

Qiao R., Dong C., Ji S., Chang X. (2021) Spatial Scale Effects of the Relationship between Fractional Vegetation Coverage and Land Surface Temperature in Horqin Sandy Land, North China. *Sensors (Basel)* 21 (20): 6914.

Rashki A., Arjmand M., Kaskaoutis D.G. (2017) Assessment of dust activity and dust plume pathways over Jazmurian Basin, southeast Iran. *Aeolian Res.* 24:145–160.

Zeidali A., Barani H., Hosseinali Zadeh M. (2015) Assessment of Dust Impact on Rangeland and Livestock Production According to Ranchers Opinion (Case Study: Andimeshk District, Iran). *Journal of Rangeland Science* 5 (4): 303–312.